

## Validation of Computational Models of Steel-Concrete Composite Beams<sup>1)</sup>

Agnieszka PEŁKA-SAWENKO<sup>1)</sup>, Tomasz WRÓBLEWSKI<sup>1)</sup>,  
Maciej SZUMIGAŁA<sup>2)</sup>

<sup>1)</sup> *West Pomeranian University of Technology of Szczecin*  
*Faculty of Civil Engineering and Architecture*

Piastów 50, 70-311 Szczecin, Poland  
e-mail: {aps, wroblewski}@zut.edu.pl

<sup>2)</sup> *Institute of Structural Engineering*  
*Poznań University of Technology*

Piotrowo 5, 60-965 Poznań, Poland  
e-mail: maciej.szumigala@put.poznan.pl

This article discusses the process of validating computational models of steel-concrete composite beams. The validation was conducted on the basis of experimental results and covers the process of modelling and identification of selected parameters in the model. During the validation process the results of experimental studies were used, and during the experimental studies the dynamic and static parameters of composite beams were assessed. The computational model and analysis were conducted for a spatial model using the finite element method in Abaqus environment. The analysis covered the elastic performance of the beams.

**Key words:** steel-concrete composite beams, validation, Abaqus, Matlab.

### 1. INTRODUCTION

Composite constructions consist of several elements with different material parameters, permanently joined together. Typically, these include steel-concrete composite beams, used as direct and indirect elements in composite floors or as main beams in bridge girders. The basic composite beams consist of a steel section, a reinforced concrete/composite slab and a connection. Due to the role of dynamic loads applied to bridge girders and standard requirements for floor vibration control, an additional dynamic analysis is necessary.

A reliable computational model is essential both for the engineer's and scientist's work. The complexity of a model depends on the scope and precision

---

<sup>1)</sup>Paper presented at the 1st National Student's Conference BUDMIKA 2014, Poznań, April 23–25, 2014.

of the analysis it is meant to perform. Advanced computer technologies can be used to develop complex computational models and to conduct in-depth analyses, with the finite element method (FEM) being the standard method of choice [3–7]. A computational model is typically developed on the basis of basic geometric data and material parameters. Unfortunately, the results it generates are not always consistent with the real parameters of an element, especially when steel-concrete composite beams are analysed.

Almost each computational model requires validation [8–10], no matter what kind of analysis will be conducted. The paper presents the process of validation of steel-concrete composite beams using the finite element method (FEM). The process of validation was conducted on the basis of experimental results. This process consists of process modelling and identification of some parameters of models. The processes of modelling and identification were conducted on the basis of dynamic and static parameters of the steel-concrete composite beam (frequencies of normal modes, eigenmodes and deflection). After validation, the results of numerical models show high similarity to the real beam.

## 2. EXPERIMENTAL TESTS OF COMPOSITE BEAMS

Five steel-concrete composite beams with different spacing between studs (stud spacing is denoted as  $n$ ) were made and analysed. The beams are shown in Fig. 1. Steel-concrete composite beams consists of a structural steel section IPE 160 and a reinforced concrete slab ( $600 \times 60$  mm). The total length of the beam was 3200 mm. The steel section and connection slats were made from S235 steel. The reinforced concrete was made from C30/37.

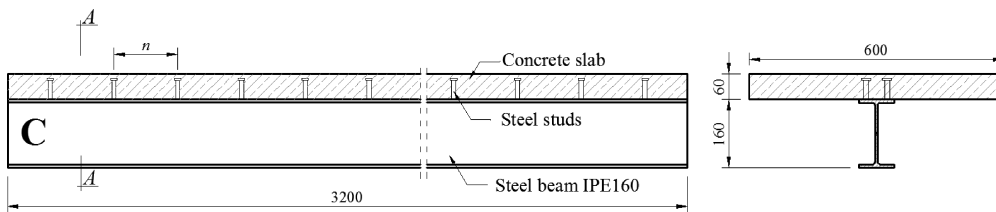


FIG. 1. Steel-concrete composite beam longitudinal view and cross-section.

The paper presents the results of analysis for beams C1, C4 and C5. Beams C2 and C3 had additional rubber bushings fixed on the studs – these results are still being analysed. The spacing between pairs of steel studs ( $n$ ) in the beams is shown in Table 1.

In the first stage of experimental tests, the basic dynamic characteristics of the beams (i.e., frequencies of natural modes, eigenmodes and damping coefficients) were analysed. The characteristics were determined for a free-end beam

**Table 1.** Types of beams and the  $n$  spacing between pairs of steel studs.

Types of beams	C1	C2	C3	C4	C5
The spacing between pairs of steel studs $n$ [mm]	200	150_g	150_g	150	100

scheme – the beam was suspended on two steel frames using steel cables. Figure 2 shows the beam on a test measuring stand. The suspension points were defined so that the system would not distort further analysis.

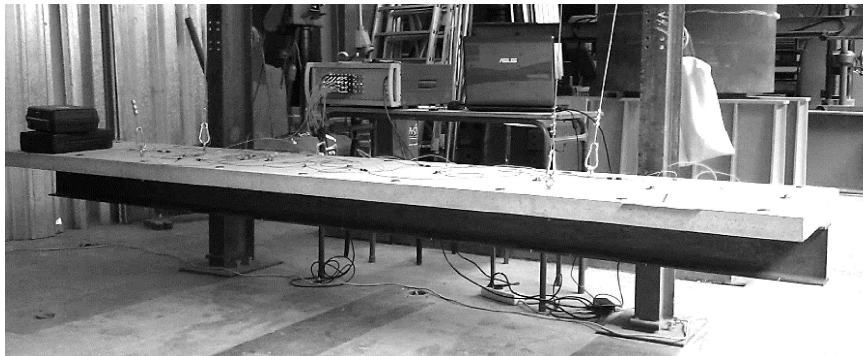


FIG. 2. Composite beam on a dynamic parameter test stand.

This phase involved impulse excitation technique and acceleration measurements. The tests were performed using the procedure defined in [11]. The grid of measurement points, where acceleration was recorded using triaxial piezoelectric acceleration sensors, is shown in Fig. 3. Impulse excitation was applied at points A, B and C – in Fig. 3 the points are marked as x. Based on the results of dynamic tests, some parameters of the models were identified. An additional analysis of the dynamic characteristics of the IPE 160 steel section, 320 mm in

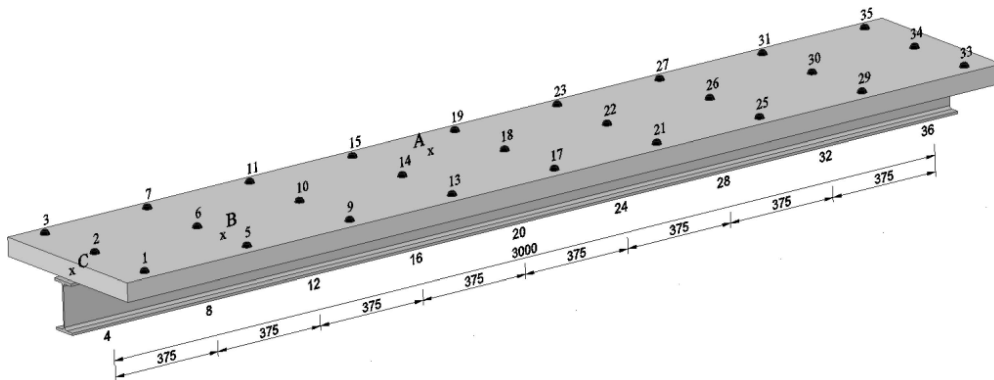


FIG. 3. Measurement points for composite beams.

length, was conducted. The scheme and excitation type were the same as those for the composite beam.

The second stage of the experimental tests was the analysis of the beams to determine their elastic parameters under the load of 30% of their bearing capacity. The tests were conducted in the scheme of the simple beam. Bending, deflection and wedge draw-in at concrete-steel interface were analysed at selected points. The results were compared with those for the identified models. The beam on the measuring stand is shown in Fig. 4.



FIG. 4. Composite beam on the test stand-static load.

### 3. VALIDATION OF THE COMPUTATIONAL MODELS

The process of validation allows to estimate the degree of similarity between the computational model and the real work of particular/certain/chosen elements. The validation process of computational model consists of several analyses of the model, i.e., the process of modelling of an element (definition of the basic geometric parameters and the material constants), preliminary verification of the model, selection of the elements with parameters having a significant influence on the work of model and the identification of selected parameters in the model, which will be analysed in the following paragraphs.

#### *3.1. Development and analysis of FEM models of composite beams*

The model of steel-concrete composite beams was defined in Abaqus environment. The analysis was conducted assuming elastic behaviour of the beams. The scheme was modelled as a spatial system with independently modelled rein-

forced concrete slab, steel bar and connection. During the initial analysis of the model and its identification, the scheme of elements with free ends was assumed, and during the static analysis, the scheme of a simple beam was assumed.

Three different beam models were analysed. The first model (denoted as *Beam 1*) used solid (concrete slab) and shell elements (steel bar). In the second model (*Beam 2*), only shell elements were used. In the third model (*Beam 3*), both shell (concrete slab) and beam elements (steel bar) were used. The schemes of the three models are presented in Fig. 5. The present paper focuses on the development and validation of the solid-shell (*Beam 1*) model. The distance between the elements is the sum of half the thickness of shells that defines the top flange of steel structure and reinforced concrete slab. The process of achieving substitute stiffness of the connection in the tangential (denoted  $Kh$ ) and normal (denoted  $Kv$ ) directions was presented in [12]. The contact type definition between the elements available in the software package Abaqus was applied *Beam 1*. In this model the stiffness in both the tangential and the normal direction to the connection's plane was defined and identified.

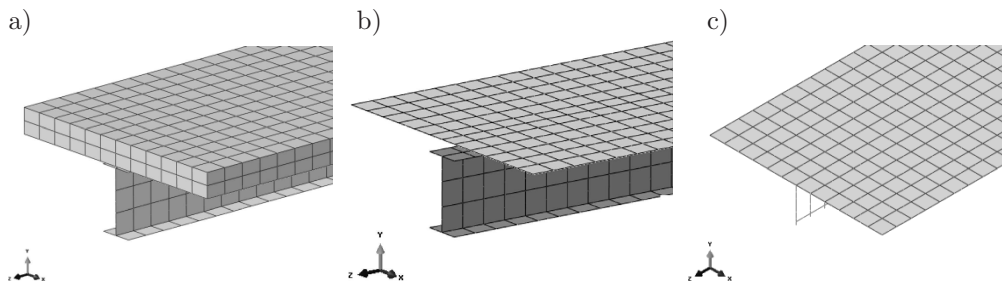


FIG. 5. The schemes of the analysed models: a) *Beam 1*, b) *Beam 2*, c) *Beam 3*.

Before the ultimate modelling of the composite beam, all its components, including the steel section and the composite slab, were analysed to account for the type and density of the finite element mesh. First, the IPE 160 steel I-beam was analysed. It was modelled with shell elements ( $M1$ ). Three layers were defined to independently model the top and bottom flanges and the web. To optimise dimensions, parameter optimisation was performed to make the equivalent section parameters close to those of the real 160 beam. The initial and final optimisation stages are presented in Table 2.

The analysis also focused on how changes of beam dynamic parameters were affected by the type of finite elements (four-node – S4R and eight-node – S8R), mesh density for the flanges and the web. The computational model results for vertical flexural vibration frequencies ( $Gv$ ), horizontal flexural vibration frequencies ( $Gh$ ) and the first axial ( $A$ ) were compared with the experimental results (Table 3).

**Table 2.** Modelled IPE 160 steel I-beam.

Dimensions	Parameters			Scheme	
	IPE 160 section	Sectional substitute		IPE 160 section	Sectional substitute
$h$ [mm]	160.0	160.0			
$b_f$ [mm]	82.0	82.0			
$t_w$ [mm]	5.0	5.0			
$t_f$ [mm]	7.4	7.6			
$R$ [mm]	9.0	-			
Parameters	Value	Value	Total error [%]		
$A_s$ [cm <sup>2</sup> ]	20.09	20.08	0.0		
$J_y$ [cm <sup>4</sup> ]	869.29	871.80	0.3		
$J_z$ [cm <sup>4</sup> ]	68.31	70.00	2.5		
$J_T$ [cm <sup>4</sup> ]	3.61	3.64	0.9		

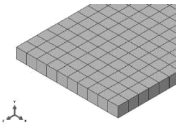
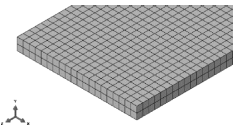
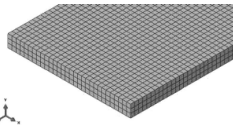
**Table 3.** Changes of normal mode frequencies in the steel section depending on finite element type and grid mesh density.

Model $\Rightarrow$	$M1\_1/S4R$	$M1\_2/S8R$	$M1\_3/S4R$	$M1\_4/S8R$	$M1\_5/S4R$						
The number of elements in the web height											
$\Rightarrow$	2		3		8						
The length of element in the length of a beam [mm]											
$\Rightarrow$	50		50		30						
The number of variables in the model / CPU time [s]											
$\Rightarrow$	2772/1.1		7878/1.8		3168/1.1						
	9060/2.1		11772/2.5								
Mode $\downarrow$	$f_{i\_exp}$ [Hz]	$f_{i\_num}$ [Hz]	Total error [%]								
1 $Gv$	113.4	110.3	2.8	112.5	0.8	111.6	1.6	112.5	0.8	112.2	1.1
2 $Gv$	295.8	288.6	2.4	293.7	0.7	291.7	1.4	293.7	0.7	292.9	1.0
3 $Gv$	541.8	527.9	2.6	535.6	1.1	532.8	1.7	535.6	1.1	534.4	1.4
4 $Gv$	824.6	803.8	2.5	813.4	1.4	810.1	1.8	813.4	1.4	811.9	1.5
1 $Gh$	32.5	28.5	12.4	32.7	-0.6	28.5	12.4	32.7	-0.6	32.3	0.6
2 $Gh$	88.9	78.3	11.9	89.5	-0.8	78.2	12.0	89.5	-0.8	88.6	0.3
3 $Gh$	171.5	152.8	10.9	173.1	-1.0	152.4	11.1	173.1	-0.9	171.6	-0.1
4 $Gh$	276.4	250.5	9.4	278.4	-0.7	248.8	10.0	278.3	-0.7	276.9	-0.2
1A	800.5	798.2	0.3	798.0	0.3	798.2	0.3	798.0	0.3	798.1	0.3
SCHEME											

Comparative analysis of the models showed that the increasing number of variables improved the consistency of computed and experimental results. For eight-node elements with square shape function (S8R), the mesh density is satisfactory (the maximum difference of 1.4%) even for the first model *M1\_2/S8R*. The four-node elements (S4R) are the linear equivalents of S8R. To obtain similar results for the model with S8R elements, the steel beam had to be divided into eight elements at the web's height, into six elements along the flanges' width and into 30 mm elements along the beam's length. For finite element mesh unification purposes, the model *M1\_5/S8R* was selected for further analysis.

The next analysed element was the reinforced concrete slab, modelled with solid elements (*model P1*). The analysis focused on changes in vertical flexural vibration frequencies (*Gv*), torsional vibration (*T*) and the first axial (*A*) of the slab depending on the type of finite element (C3D8R, C3D8I, C3D20R) and mesh density (60, 30, 20 mm). The analysis presented in Table 4 (just as above) shows that the increasing number of nodes improves the consistency

**Table 4.** Changes of normal mode frequencies in the reinforced concrete slab section depending on finite element type and grid mesh density.

Model	<i>P1/60</i>			<i>P1/30</i>			<i>P1/20</i>		
The global dimension element [mm]									
⇒	60			30			20		
Type of finite element									
⇒	C3D8R	C3D8I	C3D20R	C3D8R	C3D8I	C3D20R	C3D8R	C3D8I	C3D20R
The number of variables in the model / CPU time [s]									
⇒	3564/ 3.2	10454/ 2.4	12084/ 2.7	20412/ 7.6	76052/ 18.2	73683/ 31.4	59892/ 19.4	247092/ 62.2	222291/ 107.9
Mode ↓	$f_{i,num}$ [Hz]	$f_{i,num}$ [Hz]	$f_{i,num}$ [Hz]	$f_{i,num}$ [Hz]	$f_{i,num}$ [%]	$f_{i,num}$ [Hz]	$f_{i,num}$ [Hz]	$f_{i,num}$ [Hz]	$f_{i,num}$ [Hz]
1 Gv	2.3	20.9	20.9	18.1	20.8	20.9	19.7	20.8	20.8
2 Gv	6.3	57.2	57.4	49.8	57.4	57.4	54.2	57.4	57.4
3 Gv	12.3	111.7	112.4	97.5	112.3	112.4	106.0	112.3	112.3
4 Gv	20.2	187.7	185.4	160.7	185.0	185.2	174.7	185.1	185.1
1 T	10.1	68.1	68.9	59.8	68.7	68.7	64.9	68.7	68.7
2 T	20.3	138.6	140.3	121.8	140.0	139.9	132.0	140.0	140.0
3 T	30.8	213.6	216.6	188.0	216.0	215.9	203.9	216.0	216.0
4 T	41.7	295.0	299.9	260.2	298.9	298.9	259.9	299.0	299.0
1 A	1079.8	1079.8	1080.5	1080.3	1080.3	1080.5	1080.4	1080.4	1080.4
⇒									

of the models. The analysed solid elements were eight-node linear shape function with reduced integration (C3D8R), linear shape functions enhanced with incompatible mode function (C3D8I) and 20-node elements with square shape functions (C3D20R). Full consistency of the model for C3D8R was not achieved with the given mesh density. What is more, division into one element along the slab's height seems to produce results that completely deviate from others. This is due to integration reduced to one point in the middle of an element. Not surprisingly, such an element is not able to detect flex-induced deflection. Even for a mesh with 20 mm elements, full convergence cannot be achieved. Some eigenmodes of concrete slab were presented in Fig. 6.

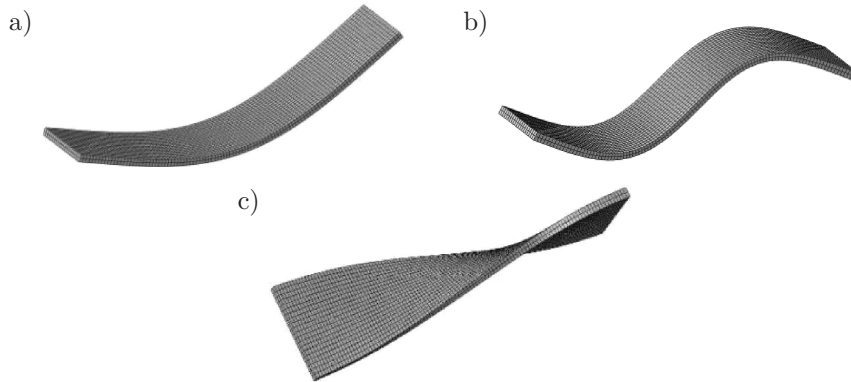


FIG. 6. Eigenmodes of concrete slab: a) first vertical flexural mode  $1 Gv$ , b) second vertical flexural mode  $2 Gv$ , c) first torsional mode ( $1 T$ ).

Very good results were obtained for C3D8I and C3D20R elements, which provided good convergence practically from the first mesh density. At the successive mesh densities (elements of 30 mm), differences between the models were almost eliminated. The time of analysis plays an important role in selecting finite elements for further analysis. Although the number of variables was similar in all the models, computation time for C3D20R was almost twice as long as that for C3D8I. Consequently, C3D8I elements were selected for further analysis. For finite element mesh unification purposes, the following parameters were finally selected: elements of 50 mm length and division into two elements at the slab's height. An additional convergence analysis of results from Table 4 confirmed the choice of mesh density.

### 3.2. Identification of the models using basic dynamic parameters

The identification process was carried out at multiple levels. The results obtained during the experimental studies for basic dynamic and static parameters of the steel-concrete composite beams were analysed.

The first stage (*STAGE 1*) of identification was conducted on the basis of experimental test of dynamic parameters. The first parameter was the dynamic longitudinal modulus of elasticity of the concrete slab  $E_d$ , accounting for the effect of its longitudinal reinforcement. The other two parameters concerned the stiffness of connection, which plays an important role in composite structures. In dynamic analysis, it is necessary to have stiffness in the direction tangential to the plane of connection ( $K_{Hz}$ ) and connection stiffness in the direction normal to the plane of connection ( $K_v$ ).

Identification of the models was limited to four flexural and one axial eigenmodes. The best fit of computational and experimental dynamic characteristics was assumed to be the consistency criterion. Consequently, index  $S_d$  can be minimised and can be given by

$$(3.1) \quad S_d = \sum_{I=1}^5 \left( \frac{f_{i\_flex}^{exp} - f_{i\_flex}^{com}}{f_{i\_flex}^{exp}} \right)^2 + \left( \frac{f_{1\_long}^{exp} - f_{1\_long}^{com}}{f_{1\_long}^{exp}} \right)^2,$$

where  $S_d$  is the dynamic sum of squares of relative deviations of computational and experimental frequencies of the first five modes of flexural vibrations and fundamental mode of axial vibration,  $f_{i\_flex}$  – next flexural vibrations,  $f_{1\_long}$  – frequency of fundamental mode of axial vibration, exp – experimental results and com – computational results.

Parameter identification and analysis of the computational model were conducted using an automatic computational loop, combining optimset tool in Matlab, Python and Abaqus environments. Identification results are presented in Table 5. During the first stage of the analysis the similarity between computational and real vectors of the form of vibrations was controlled. Some eigenmodes of steel-concrete composite beam are presented in Fig. 7.

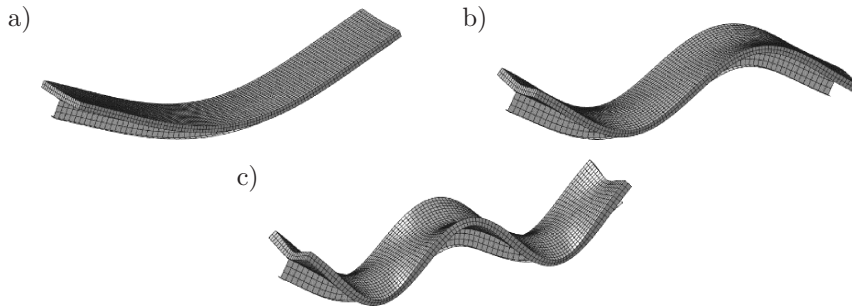


FIG. 7. Eigenmodes of beam: a) the first flexural mode 1  $Gv$ , b) the second flexural mode 2  $Gv$ , c) the third flexural mode 3  $Gv$ .

**Table 5.** Identification results of the steel-concrete beams.

Mode ↓	$f_{i\_exp}$ [Hz]	$f_{i\_num}$ [Hz]	Total error $\Delta$ [%]
<b>BEAM C_1</b>			<b>STAGE 1</b>
1 <i>Gv</i>	76.6	77.2	-0.8
2 <i>Gv</i>	178.4	177.5	0.5
3 <i>Gv</i>	283.0	283.1	0.0
4 <i>Gv</i>	383.5	384.1	-0.2
1A	626.8	620.5	1.0
$S_d$		$2.144E-04$	
$E_d$ [N/m <sup>2</sup> ]		3.218E+10	
$K_v$ [N/m <sup>3</sup> ]		4.000E+10	
$K_h$ [N/m <sup>3</sup> ]		4.255E+10	
<b>BEAM C_4</b>			<b>STAGE 1</b>
1g	77.2	77.5	-0.3
2g	178.0	177.8	0.1
3g	283.1	283.7	-0.2
4g	386.1	385.9	0.1
1o	632.2	629.4	0.4
$S_d$		$1.459E-04$	
$E_d$ [N/m <sup>2</sup> ]		3.324E+10	
$K_v$ [N/m <sup>3</sup> ]		3.882E+10	
$K_h$ [N/m <sup>3</sup> ]		3.926E+10	
<b>BEAM C_5</b>			<b>STAGE 1</b>
1g	78.2	78.8	-0.8
2g	183.7	184.2	-0.3
3g	295.7	296.9	-0.4
4g	405.9	405.7	0.1
1o	650.5	643.6	1.1
$S_d$		$2.622E-04$	
$E_d$ [N/m <sup>2</sup> ]		3.722E+10	
$K_v$ [N/m <sup>3</sup> ]		5.080E+10	
$K_h$ [N/m <sup>3</sup> ]		6.754E+10	

### 3.3. Identification of the models using basic static parameters

The next *STAGE2* of identification was conducted using the results of experimental tests, by comparing model response to the given load. Loads induced

into the model (points and forces) were the same as those induced into the beam in the tests. The boundary conditions of the model were the same as those for the simple beam in the experiments. The force of 1.5 kN was applied to the beam with 1 m spacing. Deflection was measured in points P1, P2 and P3 that overlapped with the points selected in the tests. Next, deflection values  $u_{i\_exp}$  recorded in the experiments were compared with those  $u_{i\_num}$  obtained from the computational model. The loading scheme and measurement points are presented in Fig. 8.

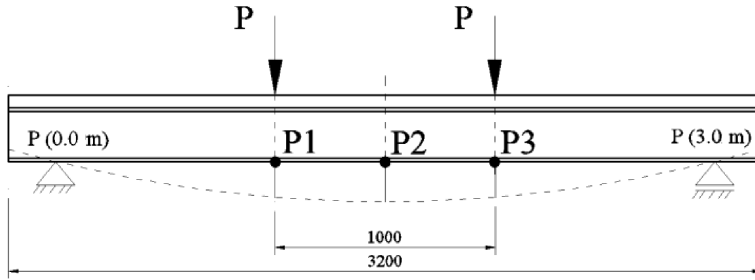


FIG. 8. Loading scheme, measurement points of beam deflection.

The second step (*STAGE 2*) of identification decomposed for two cases (*STAGE 2a* and *STAGE 2b*). At the *STAGE 2a*, identification data were analysed, with the dynamic longitudinal modulus of elasticity  $E_d$ . At the *STAGE 2b*, an attempt was made to estimate the static modulus of elasticity  $E_c$ , based on modulus  $E_d$ . In line with the guidelines in [13] and [14], the relation between the moduli can be given by

$$(3.2) \quad E_c = 1.25 \cdot E_d - C,$$

where constant  $C$  was determined for concrete types in which cement content does not exceed  $500 \text{ kg/m}^3$ .

During the *STAGE 2* the index  $S_s$  can be given by

$$(3.3) \quad S_{s/i} = \sum_{j=1}^3 \left( \frac{u_j^{\text{exp}} - u_j^{\text{com}}}{u_j^{\text{exp}}} \right)^2,$$

where  $S_s$  is the static sum of squares of relative deviations of computational and experimental deflection of the beam,  $I$  – index  $a$  or  $b$  depending on the *STAGE* of the identification,  $u_j$  – value of deflection in the point, exp – experimental results and com – computational results.

Identification results for beams C1, C4 and C5 for *STAGE 2a* and *STAGE 2b* are presented in Tables 6, 7, and 8, respectively.

**Table 6.** Identification results for beam C1 for *STAGE 2a* and *STAGE 2b*.

Analysis	Static			Dynamic	
Point ↓	$u_{i\_exp}$ [mm]	$u_{i\_num}$ [mm]	Total error [%]	Mode ↓	$f_{i\_num}$ [Hz]
<b>Beam C_1</b>			<b>STAGE 2a</b>		
P1	3.06	2.83	7.5	1 <i>Gv</i>	38.25
P2	3.52	3.22	8.4	2 <i>Gv</i>	121.24
P3	3.03	2.83	6.6	3 <i>Gv</i>	186.19
$S_{s/2a}$		1.71E-2		1A	667.94
$E_d$ [N/m <sup>2</sup> ]		3.218E+10			
<b>Beam C_1</b>			<b>STAGE 2b</b>		
P1	3.06	3.11	-1.5	1 <i>Gv</i>	36.55
P2	3.52	3.54	-0.7	2 <i>Gv</i>	116.15
P3	3.03	3.11	-2.5	3 <i>Gv</i>	178.36
$S_{s/2b}$		9.02E-4		1A	598.88
$E_{cm}$ [N/m <sup>2</sup> ]		2.123E+10			

**Table 7.** Identification results for beam C4 for *STAGE 2a* and *STAGE 2b*.

Analysis	Static			Dynamic	
Point ↓	$u_{i\_exp}$ [mm]	$u_{i\_num}$ [mm]	Total error [%]	Mode ↓	$f_{i\_num}$ [Hz]
<b>Beam C_4</b>			<b>STAGE 2a</b>		
P1	3.06	2.81	8.2	1 <i>Gv</i>	38.381
P2	3.52	3.21	8.8	2 <i>Gv</i>	121.41
P3	3.03	2.81	7.3	3 <i>Gv</i>	186.42
$S_{s/2a}$		1.97E-2		1A	675.6
$E_d$ [N/m <sup>2</sup> ]		3.324E+10			
<b>Beam C_4</b>			<b>STAGE 2b</b>		
P1	3.06	3.07	-0.3	1 <i>Gv</i>	36.82
P2	3.52	3.51	0.4	2 <i>Gv</i>	116.74
P3	3.03	3.07	-1.3	3 <i>Gv</i>	179.28
$S_{s/2b}$		1.93E-4		1A	592.9
$E_{cm}$ [N/m <sup>2</sup> ]		2.123E+10			

In computational models of *Beam C\_5*, deflection differences were about 7%, which may suggest some inconsistencies in the model. The whole process of model development and model identification should be analysed again at length.

**Table 8.** Identification results for beam C5 for *STAGE 2a* and *STAGE 2b*.

Analysis	Static			Dynamic	
Point ↓	$u_{i\_exp}$ [mm]	$u_{i\_num}$ [mm]	Total error [%]	Mode ↓	$f_{i\_num}$ [Hz]
<b>Beam C_5</b>			<b><i>STAGE 2a</i></b>		
P1	3.06	2.69	12.1	<i>1 Gv</i>	38.935
P2	3.52	3.07	12.8	<i>2 Gv</i>	124.74
P3	3.03	2.69	11.2	<i>3 Gv</i>	191.42
$S_{s/2a}$		4.36E-2		<i>1A</i>	703.86
$E_d$ [N/m <sup>2</sup> ]		3.722E+10			
<b>Beam C_5</b>			<b><i>STAGE 2b</i></b>		
P1	3.06	2.87	6.2	<i>1 Gv</i>	37.72
P2	3.52	3.28	6.8	<i>2 Gv</i>	120.70
P3	3.03	2.87	5.3	<i>3 Gv</i>	185.47
$S_{s/2b}$		1.13E-2		<i>1A</i>	592.52
$E_{cm}$ [N/m <sup>2</sup> ]		2.753E+10			

The same applies to the real model. During further analysis, this model will be removed.

#### 3.4. Validation of the computational models – the global degree of similarity

The global degree of similarity  $S_G$  of computational model for the composite beam, expressed in percent, can be given by

$$(3.4) \quad S_{G/i} = 1 - (S_d + S_{s/i}),$$

where  $i$  – index  $a$  or  $b$  depending on the *STAGE* of the identification,  $S_d$  – dynamic results sum of squares – *STAGE 1* and  $S_s$  – static sum of squares depending on the *STAGE* –  $a$  or  $b$ .

The final values of  $S_G$  are presented in the fourth row of Table 9. The global error between the results obtained in *STAGE 2a* and *2b* is denoted as  $E_{TOT}$ , the values are presented in the third row of Table 9.

**Table 9.** The global degree of similarity  $S_G$  of computational model for composite beam.

No	Description		<i>Beam C_1</i>	<i>Beam C_4</i>
1	$S_d + S_{s/2a}$	<i>STAGE 1 + STAGE 2a</i>	<i>1.73E-02</i>	<i>1.98E-02</i>
2	$S_d + S_{s/2b}$	<i>STAGE 1 + STAGE 2b</i>	<i>1.12E-03</i>	<i>3.48E-04</i>
3	$E_{TOT}$	The global error	94%	98%
4	$S_G$	The global degree of similarity	<b>99.89%</b>	<b>99.97%</b>

#### 4. CONCLUSIONS

The processes of development and validation of computational models of the steel-concrete composite beam were presented. Beams models were defined in FEM as a spatial system using Python, Abaqus and Matlab systems. After validation, the results of *Beam C\_1* and *Beam C\_2* numerical analyses show high similarity to real steel-concrete beams.

The identification process was carried out at a multi-level using the results of the experimental studies. The *STAGE 1* of identification was based on the results of experimental research defining the dynamic parameters of the beams. *STAGE 1* was performed using equivalent section, material parameters and connection stiffness. The process of identification was carried out on experimental results, determining the dynamic parameters of the beams. On balance, identification was successful and the maximum difference between results obtained for all the beam models was 1.1%.

The *STAGE 2* of identification was based on the results of experimental research defining the static parameters of the beams. Summing up the analysis of *STAGE 2* it can be concluded that the change of the static modulus of elasticity  $E_c$  had a positive impact on the degree of similarity of the models. The computational models of *Beams C1* and *C4* showed high convergence to the real model.

#### ACKNOWLEDGMENT

This research work was co-financed by the European Union under the European Social Fund and the State Budget, the Operational Programme Human Capital Priority VIII, Measure 8.2 “Transfer of knowledge”, Sub-measure 8.2.2 “Regional Innovation Strategies” within the system project implemented by the Regional Labour Office in Szczecin “An investment in knowledge as a driving force for development of innovation in the region – third edition”.

#### REFERENCES

1. Abaqus Theory Manual. Version 6.13, ABAQUS Inc., 2013.
2. Abaqus Analysis User’s Manual. Version 6.13, ABAQUS Inc., 2013.
3. LUO Y., LI A., KANG Z., *Parametric study of bonded steel-concrete composite beams by using finite element analysis*, Engineering Structures, **34**: 40–51, 2012.
4. PRAKASH A., ANANDAVALLI N., MADHESWARAN C.K., RAJASANKAR J., LAKSHMANAN N., *Three dimensional FE model of stud connected steel-concrete composite girders subjected to monotonic loading*, International Journal of Mechanics and Applications, **1**(1): 1–11, 2011.

5. THEVENDRAN V., SHANMUGAM N.E., CHEN S., LIEW R.J.Y., *Experimental study on steel-concrete composite beams curved in plan*, Engineering Structures, **22**(8): 877–889, 2000.
6. MIRZA O., UY B., *Behaviour of headed stud shear connectors for composite steel-concrete beams at elevated temperatures*, Journal of Constructional Steel Research, **65**(3): 662–674, 2009.
7. VASDRAVELLIS G., UY B., TAN E.L., KIRKLAND B., *The effects of axial tension on the hogging-moment regions of composite beams*, Journal of Constructional Steel Research, **68**(1): 20–33, 2012.
8. UHL T., *Computer-assisted identification of models of mechanical structures* [in Polish], Wydawnictwa Naukowo-Techniczne, Warszawa, 1997.
9. ABRAMOWICZ M., BERCZYŃSKI S., WRÓBLEWSKI T., *Estimation of the parameters of the discrete model of a reinforced concrete slab*, 11th International Conference on Vibration Problems, Z. Dimitrovová et al. [Eds.], Lisbon, Portugal, September 2013.
10. PEETERS B., LOWET G., VAN DER AUWERAER H., LEURIDAN J., *A new procedure for modal parameter estimation*, Sound and Vibration, **38**(1): 24–28, 2004.
11. BERCZYŃSKI S., WRÓBLEWSKI T., *Experimental verification of natural vibration models of steel-concrete composite beams*, Journal of Vibration and Control, **16**(9): 2057–2081, 2010.
12. PEŁKA-SAWENKO A., ABRAMOWICZ M., WRÓBLEWSKI T., BERCZYŃSKI S., SZUMIGAŁA M., *Modeling and analysis of free vibration of steel-concrete composite beams*, [in] Recent Advances in Computational Mechanics, T. Łodygowski, J. Rakowski, P. Litewka [Eds.], CRC Press/Balkema, 103–110, Boca Raton, London, New York, Leiden, 2014.
13. NEVILLE A.M., *The properties of concrete* [in Polish], Polski Cement, Kraków, 2000.
14. British Standards Institution (BSI) CP 110, *Code of practice for structural use of concrete: part 1 – design, materials and workmanship*, London, 1972.

*Received July 17, 2014; accepted version June 5, 2015.*

---